Three-Pulse Photon Echo Measurements on LH1 and LH2 Complexes of *Rhodobacter sphaeroides*: A Nonlinear Spectroscopic Probe of Energy Transfer

Ralph Jimenez,[†] Frank van Mourik,[‡] Jae Young Yu,[†] and Graham R. Fleming*,[†]

Department of Chemistry and the James Franck Institute, The University of Chicago, 5735 South Ellis Avenue, Chicago, Illinois 60637, and Department of Physics and Astronomy, The Free University of Amsterdam, de Boelelaan 1081, 1081 HV Amsterdam, The Netherlands

Received: January 23, 1997; In Final Form: April 8, 1997[⊗]

Three-pulse echo peak shift measurements were performed on the B875 and B850 bands of detergent-isolated LH1 and LH2 complexes at room temperature. The peak shifts are much larger and decay much faster than typically observed for dye molecules in solution. Simulations of the peak shifts based on the optical transition frequency correlation function, *M(t)*, are presented. *M(t)* includes contributions from rapid protein fluctuations, vibrational motion, and energy transfer. The model reproduces the room temperature absorption spectra of B850 and B875, shows that the coupling of electronic and nuclear degrees of freedom is much weaker than for dyes in solution, and identifies contributions to the line shapes that may be important to the energy transfer processes. The implications of these results for the extent of electronic delocalization in LH1 and LH2 are also discussed. Although the role of coherence transfer still needs to be understood, the results are shown to be consistent with the use of weak-coupling excitation transfer models of B850 and B875.

I. Introduction

In photosynthesis, most of the light energy is absorbed by antenna complexes and then transferred to the reaction center with very high overall efficiency. The absorbed energy migrates over many pigments as an electronic excitation before being trapped by the reaction center in a process whose overall time scale is ∼50 ps.[1] The individual excitation transfer steps, therefore, occur on subpicosecond time scales.

In photosynthetic purple bacteria, there are two types of light-harvesting antenna, core (LH1) and peripheral (LH2) light-harvesting complexes. The chromophores in LH1 and LH2 are bacteriochlorophylls (Bchl) and carotenoids. Here, we will focus on the dynamics of the Bchl pigments in bacteriochlorophyll *a*-containing bacteria. The LH1 complexes contain only one type of Bchl absorbing at ∼875 nm (B875), whereas LH2 complexes contain two types of Bchl, absorbing at 800 nm (B800) and 850 nm (B850). Recently, high-resolution crystal structures of some LH2 complexes have become available. The α-helices of the protein coordinate the Bchl into ringlike structures with very small distances between pigments.[2] For example, the crystal structure of LH2 from *Rhodopseudomonas acidophila* shows a basic unit with 9-fold symmetry.[3] The $\alpha\beta$-polypeptides coordinate 18 B850 pigments into a closely interacting ring. The spacing between the chlorin rings is slightly staggered, alternating between 3.5 and 3.9 Å.[4] The B800 pigments are separated by ∼21 Å, and the closest approach between B800 and B850 is 17.6 Å. The crystal structure of LH2 from *Rhodospirillum molischianum* shows similar features in a ring with 8-fold symmetry.[5] Two-dimensional electron diffraction of LH1 reveals a larger ring very similar to B850 with 32 Bchl, possibly segregated into pairs.[6] However, the resolution of this study is not sufficient to specify precisely the distances between pigments.

1. Related Work. Many time-resolved studies have focused on determining the time scale of excitation transfer within these complexes at room temperature. Pump−probe techniques have been used to study B800 to B800 and B800 to B850 excitation transfer.[7−9] In LH2, excitation transfer from B800 to B850 takes 600−700 fs at room temperature.[7,8,13] Transfer within the B800 group of cofactors takes approximately 700 fs.[9] Since the distances separating the pigments are large compared to the dimensions of the Bchl molecules, these processes are probably well described with weak-coupling theories of energy transfer such as Förster theory.[10] The mode of energy transfer within the B850 and B875 pigments is less clear, because the electronic structure of these aggregates is not yet well understood. One line of thought is suggested by the finding that the LH1 antenna can be reversibly dissociated into a subunit that has the properties of a strongly interacting dimer of Bchl.[11] This result has prompted the hypothesis that excitation transfer within B850 and B875 can be described as hopping from dimer to dimer.[12,13,23] The extent to which this picture is accurate, or whether larger degrees of delocalized excitation (excitons) must be considered, are topics of current debate. For example, Sauer and co-workers have performed calculations of the optical absorption and circular dichroism (CD) spectra of LH2, using the crystallographic coordinates of *Rps. acidophila*.[20] From simulations of the CD spectra, they suggest that the B850 electronic state is delocalized over nearly the entire ring at room temperature. Kennis *et al.* have measured subpicosecond absorbance difference spectra of LH2 complexes from *Rhodobacter sphaeroides* and *Chromatium tepidum* in which they interpret the unusually large absorbance changes in B850 (which are a factor of 4 larger than in B800) to be the result of excitation delocalized over the whole ring.[17] In another experimental study, Pullerits *et al.* have modeled their absorbance difference spectra of B850 from *Rb. sphaeroides* with an exciton calculation including two excited electronic states of each Bchl.[18,19] By fitting the shape of the spectral features, they conclude the excitation to be delocalized over 4 ± 2 Bchl. Monshouwer *et al.* measured the radiative rate of LH1 and LH2 and found values that are a factor of 2−3 higher than monomeric Bchl.[21] None of these studies modeled

* To whom correspondence should be addressed. Permanent address: Department of Chemistry, University of California, Berkeley, Berkeley, CA 94720.
[†] The University of Chicago.
[‡] The Free University of Amsterdam.
[⊗] Abstract published in *Advance ACS Abstracts,* August 15, 1997.

S1089-5647(97)00299-X CCC: $14.00

the combined influence of vibrations and inhomogeneous broadening on the delocalization length. An attempt to consider all these effects was made in a theoretical study in which the extent of delocalization was calculated by a Green's function approach as a function of electronic coupling, homogeneous line width, and inhomogeneous width.[22]

Recently, fluorescence depolarization measurements have been performed on the LH1 and LH2 complexes of *Rb. sphaeroides*.[12,13] These studies interpreted the time scale of depolarization in terms of site-to-site hopping within the ringlike structures suggested by crystallography, thus revealing the time scale of the hopping process. For both B875 and B850, multiexponential depolarizations were observed. For example, in LH1 time constants of approximately 100 and 500 fs with relative amplitudes of 70% and 30% were observed.[12] In B850 a somewhat shorter initial decay of ∼50 fs was observed (70%) followed by a 500 fs anisotropy decay.[13] In both cases the initial values were near 0.4 and decayed to asymptotic values near 0.1, indicating randomization of the excitation in a plane. These results were modeled by assuming Förster excitation transfer from dimer to dimer in isolated rings where the site energies follow a Gaussian distribution around the absorption maximum. The average hopping times resulting from this model are on the order of 100 fs. Reasonable agreement between the model and data were obtained for a homogeneous line width of 250 cm^{-1} for the dimeric subunits and a 500 cm^{-1} fwhm distribution of dimer absorption energies. In the case of LH1, these values are in reasonable agreement with the ∼580 cm^{-1} fwhm of the room temperature absorption spectrum. The difference in depolarization times in this model mainly reflects the difference in ring sizes between LH1 and LH2, not a difference in hopping rates. Precise determination of the hopping rate requires knowledge of the ring size and a monodisperse sample, as well as a method with higher time resolution. A simple exciton calculation was performed for B850 by assuming coupling strengths of 230 and 110 cm^{-1} for the intradimer and interdimer electronic interactions and a 200 cm^{-1} Gaussian distribution of site energies.[13,14] The calculated exciton level structure was in good agreement with the observed width of the $k = 0$ level in low-temperature hole burning.[15] Furthermore, calculation of the inverse participation ratio on the low-energy side of the band gave a value of ∼0.25, i.e., an excitation delocalized over four pigments. Similar conclusions were reached for LH1.[12] These calculations only considered the effects of static disorder; i.e., phonons were ignored. It was, therefore, suggested that the combined influence of static disorder and vibrations will localize the excitation onto a dimer, thereby validating the hopping model.[12,13] The manner in which delocalized states would manifest themselves in these experiments, however, is still under investigation.

Another type of measurement that has given information on the extent of inhomogeneous broadening in these systems is broad-band time-resolved pump−probe.[23,24] In these experiments, the LH1 antenna of *Rb. sphaeroides* and *Rhodospirillum rubrum* were nonselectively excited in the Q_x spectral region. As a result of energy transfer from higher energy pigments to lower energy pigments within the band, the excitation will approach a thermal distribution. This equilibration process was measured by tracking the zero-crossing point of the transient spectrum, which, in *Rb. sphaeroides* LH1, shifts ∼140 cm^{-1} lower in energy with a 700 fs time constant.[24] This observation can be explained with a model almost identical to that used for modeling the fluorescence depolarization. The magnitude and time constant of the spectral shift are consistent with a ratio of homogeneous/inhomogeneous width of ∼0.6, consistent with the values obtained from the depolarization simulations.

Thus far, studies have assumed a weak-coupling Coulombic (Förster) approach to calculating the energy transfer rates. In the cases of B850 and B875 dynamics, this assumption is called into question by various observations. (1) The ∼100 fs hopping times from these models imply rather large values of electronic coupling, taking the situation in these complexes outside the realm of applicability of the very weak coupling model considered by Förster.[10] (2) As mentioned already, the high-resolution crystal structures do not reveal distinct segregation of the Bchl into monomers, dimers, etc. Instead, the excitations are thought to be localized as a result of energetic and dynamical considerations. A proper description of energy migration in these complexes should make a natural transition between exciton and hopping models as a function of electronic coupling, static disorder, and dynamical factors (i.e., spectral density of fluctuations). (3) For both LH1 and LH2, coherent vibrational motion has been observed on time scales that far outlast the putative hopping times. Förster theory assumes vibrationally dephased, relaxed chromophores. In light of these observations, a Förster approach may not apply to energy transfer in B850 and B875. A full description of excitation transfer in these systems must include coherence transfer. The development of Redfield theory for coherent condensed phase reactive dynamics is being pursued by Jean.[27−29] Evidently, a complex mechanism of energy transfer applies to these systems.

The roughly 500-fold ratio between the estimated hopping times (∼ 80 fs) in LH1 and the overall time scale for trapping at the reaction center in LH1-only mutants of 50 ps invokes the notion of a "storage ring" though, of course, we do not mean to imply a unidirectional energy flow in the ring.[30,31] For such a storage ring to function efficiently, weak coupling between the electronic and nuclear degrees of freedom seems necessary to avoid excessive dissipation of the excitation energy. In a system of noninteracting chromophores, the gap between the steady state absorption and emission spectra (the Stokes shift) gives a direct estimate of the overall strength of coupling of the electronic transition with the nuclear degrees of freedom (i.e., the total reorganization from both solute and solvent). However, in an inhomogeneous system with energy transfer, the progressive red shift of the emission as the excitation "equilibrates" over the distribution makes it difficult to obtain a similar estimate of the reorganization energy. The three-pulse echo peak shift (3PEPS) measurements described in this work show that the overall reorganization is small in both B850 and B875 compared to chromophores in solution or polymer glasses.[38,37]

2. The 3PEPS Experiment. In this section we provide a brief description of the three-pulse echo peak shift measurement in order to elucidate the likely molecular contributions to our signals. Detailed descriptions of the experiment are given elsewhere.[32] As Figure 1 shows, there are three time periods of concern here. The first time period, τ, in which the system is in an electronic superposition state, is scanned. During the second time period, T, the system is in a diagonal (population) state. This is the key point that gives the measurement its large dynamic range, extending from a few femtoseconds to hundreds of picoseconds. During the last time period, the system is in a coherence until the echo emerges. The detector integrates over the final time interval by recording the echo intensity along the phase matching direction. The observable of interest is the location of the echo maximum (obtained by scanning τ) with respect to zero delay for different fixed values of T, the population period (i.e., the "peak shift"). As discussed in ref 35, when the inhomogeneous broadening is neither extremely large nor extremely small, the shift of the echo maximum from zero, $\tau^*(T)$, at a particular value of T reflects the extent to which rephasing is still possible. In other words, the peak shift reflects the degree of retained memory of the initial transition frequency.

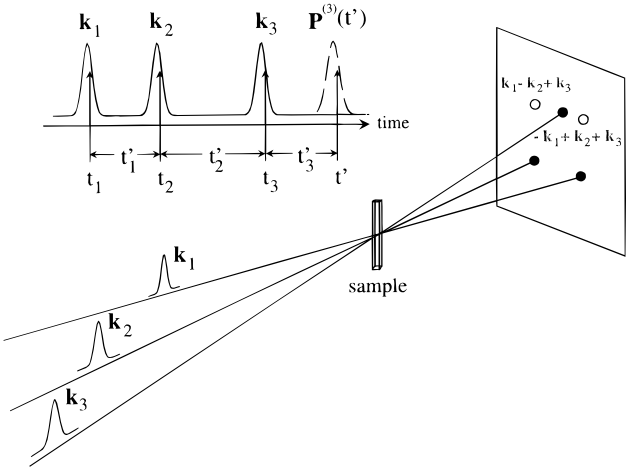

Figure 1. Pulse sequence and phase matching diagram for the three-pulse echo. The three pulses, incident on the sample with wave vectors $\mathbf{k}_1$, $\mathbf{k}_2$, and $\mathbf{k}_3$, generate two mirror-image echo signals in the phase matched directions $\mathbf{k}_1 - \mathbf{k}_2 + \mathbf{k}_3$ and $-\mathbf{k}_1 + \mathbf{k}_2 + \mathbf{k}_3$, as indicated in the diagram by the open circles. The experimentally controllable center-to-center temporal delays between $\mathbf{k}_1$ and $\mathbf{k}_2$ and between $\mathbf{k}_2$ and $\mathbf{k}_3$ are τ and T, respectively. These two delays are sometimes referred to as the coherence and population times. For the purposes of calculation, t_1, t_2, and t_3 denote field-matter interaction points, while t_1', t_2', and t_3' refer to delays between interaction points (see eq 9). $\mathbf{P}^{(3)}(t')$ is the third-order polarization generated by the three interactions at t_1', t_2', and t_3.

In a system without energy transfer, both dynamical and static contributions to the line width are reflected in the form of $\tau^*(T)$ vs T. Static inhomogeneity means that some rephasing will be possible even at long times; only when the memory of the transition frequency is completely lost will $\tau^*(T) = 0$.

In general, the memory of the electronic transition frequency can be written as a time correlation function. For the case of noninteracting molecules in solvents, the peak shift has been shown to reveal time scales in the time correlation function of the electronic transition frequency, *M(t)*:[35]

$$M(t) = \frac{\langle \Delta\omega(0)\, \Delta\omega(t) \rangle}{\langle \Delta\omega^2 \rangle} \tag{1}$$

where $\Delta\omega(t)$ is the fluctuating part of the electronic transition frequency for each chromophore, referenced to its central frequency,

$$\omega_i(t) = \Delta\omega(t) + \langle\omega\rangle + \epsilon_i \tag{2}$$

where ϵ_i is the static offset (taken from the inhomogeneous distribution) and $\langle\omega\rangle$ is the average electronic transition frequency.[43] For a typical dye molecule in solvent at room temperature, *M(t)* is a sum of Gaussian (inertial), exponential (diffusive), and oscillatory (inter- and intramolecular vibrational) contributions.[43] *M(t)* does not make a distinction between modes of the protein environment and vibrational modes of the chromophores.

To extract quantitative values of the parameters from peak shift data requires extensive numerical modeling.[32,33] However, the physical content of the experiment can be appreciated via two approximate expressions valid only (a) at high temperatures, (b) for times longer than the bath correlation time, and (c) for intermediate inhomogeneous broadening ($\Delta_{in} < \Gamma$, see ref 35 for details).

$$\tau^*(T) = \frac{\sqrt{\Gamma + \Delta_{in}^2 + f(T)}\,(\Gamma\, S(T) + \Delta_{in}^2)}{\sqrt{\pi}[\Gamma(\Gamma + 2\Delta_{in}^2 + f(T)) + \Delta_{in}^2 f(T)]} \tag{3}$$

and

$$\tau^*(T\to\infty) = \frac{\Delta_{in}^2\sqrt{\Gamma + \Delta_{in}^2 + (\lambda/\hbar)^2}}{\sqrt{\pi}[\Gamma(\Gamma + 2\Delta_{in}^2 + (\lambda/\hbar)^2) + \Delta_{in}^2(\lambda/\hbar)^2]} \tag{4}$$

where $\Gamma = 2\lambda/\hbar^2\beta$ ($\beta = 1/kT$), λ is the reorganization energy (2λ is the static Stokes shift), Δ_{in} is the fwhm of the inhomogeneous distribution, and $S(T)$ is the Stokes shift function, which at high temperature is equal to *M(t)*. Finally, $f(T) = (\lambda/\hbar)^2[1 - M(T)/M(0)]^2$. Thus, the sole dynamical quantity appearing in the peak shift is *S(t)* or *M(t)*, while at long times the peak shift is determined by the ratio of fast broadening (λ) and the static disorder (Δ_{in}). If Δ_{in} is zero, $\tau^*(T\to\infty) = 0$, as can be readily seen from eq 4.

We now consider how expressions 3 and 4 (or the exact formulas used for data fitting) would be modified in the presence of energy transfer. The rapid processes leading to loss of memory of the transition frequency (i.e., intramolecular vibrational dynamics and inertial solvation) will still be present in the signal, as in isolated chromophores. The key difference lies in the role of the inhomogeneous broadening. This can be seen by examining eq 2. The reason that static inhomogeneous broadening allows rephasing is that individual chromophores retain memory of their transition frequencies. We are able to label each chromophore with a time-independent offset, ϵ_i, because all the optically excited chromophores remain excited. Energy transfer destroys the memory, probably on the time scale of one or a few hops, because the label i now tracks the electronically excited chromophore. Therefore, when energy transfer occurs, memory of the inhomogeneous distribution is not retained at all times: ϵ_i becomes $\epsilon_i(t)$. We, therefore, suggest that energy transfer can be incorporated by considering Δ_{in} to be time dependent; its ability to allow rephasing is progressively destroyed. The simplest assumption is that this process is exponential, and this is equivalent to adding an exponential term to *M(t)*, whose amplitude is related to the width of the distribution. The energy transfer plays a role somewhat analogous to motional narrowing. In this case it is clear that the $\tau^*(T\to\infty)$ values from these systems with extensive energy transfer cannot be used to obtain the inhomogeneous width directly. The 3PEPS experiment gives a direct measure of the homogeneous width, which in turn enables determination of the inhomogeneous width from the width of the absorption spectrum. In the absence of a more formal theory of the 3PEPS experiment in the presence of energy transfer, we take the approach outlined above for the analysis of our data.

II. Experimental Section

These experiments were performed on standard, detergent-isolated LH1 and LH2 complexes of *Rhodobacter sphaeroides*, solubilized in *N*-octyl-β-D-glucopyranoside. The samples were chilled with an ice bath and flowed through a 200 μm quartz cell with a peristaltic pump.

The laser used for these experiments is a self-mode-locked Ti:sapphire laser pumped by ~6 W from an Ar^+ laser. The mode-locked output could be tuned from ~840 to 900 nm with a razor blade inserted in the dispersed end of the cavity. The laser was cavity dumped at 250 kHz repetition rate so as to avoid the buildup of triplet Bchl in the complexes. The pulse widths were 30−35 fs at these wavelengths. The total pulse energy in each beam used for the echo measurements was in the range from 800 pJ to 1 nJ, as measured with a power meter at the sample position.

The peak shift measurement was performed as previously described, with a standard three-beam optical arrangement.[32]

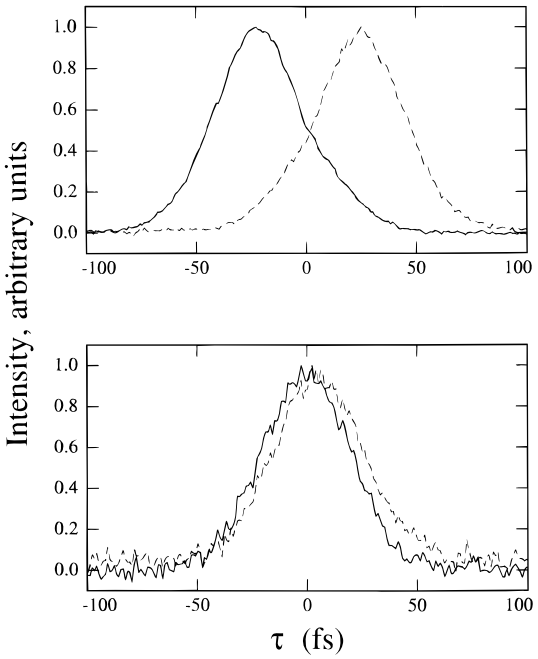

Figure 2. Three-pulse echo decays for LH1 at population delays $T = 0$ and $T = 1000$ fs, shown for the two phase matched directions. The peak shift is half the time difference between the peaks of the two echo decays at each T.

Simultaneous resolution of the two phase-matched echo signals ($\mathbf{k}_1 - \mathbf{k}_2 + \mathbf{k}_3$ and $-\mathbf{k}_1 + \mathbf{k}_2 + \mathbf{k}_3$) allows precise determination of the peak shift (error bars ± 0.3 fs). In order to minimize scatter, two beams were chopped, and lock-in detection of the diode signals at the difference frequency was employed. The beams were focused into the sample by a 20 cm achromatic lens to avoid large crossing angles between beams which may result in an artificial residual peak shift.[37,38] It was verified that the peak shift for IR144 in DMSO was <1 fs at population delays >25 ps. This observation is important for the interpretation of residual peak shift values.

Normally, the three-pulse echo peak shift measurement is performed with all polarizations parallel to each other. In this study, we have an interesting situation where the excitation moves among chromophores whose transition moments are not parallel. One might anticipate polarization effects on the echo signals. The typical coherence period (see Figure 1) is of a duration comparable or smaller than the observed depolarization times. However, the population periods are often of much longer duration. We set the polarizations of the first two pulses parallel to each other and varied the polarization of the third pulse ($\mathbf{k}_3$) from parallel to magic angle. We found only a small effect on the peak shift as a result of the polarization changes. The magnitude of the peak shift decreased by ~1 fs or less at all times when rotating the polarization from parallel to magic angle, and the time scales of the decays were not affected.

III. Results and Discussion

The LH1 and LH2 transient absorption, transient grating, and three-pulse echo signals were measured in this study. Representative LH1 three pulse echo decays for population times of $T = 0$ fs and $T = 1000$ fs are shown in Figure 2. The LH1 and LH2 peak shifts, each measured with the polarization of $\mathbf{k}_3$ at magic angle, are shown in Figure 3.

As a starting point for discussion, we note the interesting features of these peak shift decays. (1) The initial values of the peak shifts (~24 fs) are in both cases significantly larger than typically observed for dyes.[32,38] (2) The peak shift decays are 90% complete in <250 fs. (3) Smaller amplitude (10%) decay components on much longer time scales are present (see inset to Figure 3). Our analysis will attempt to explain these features.

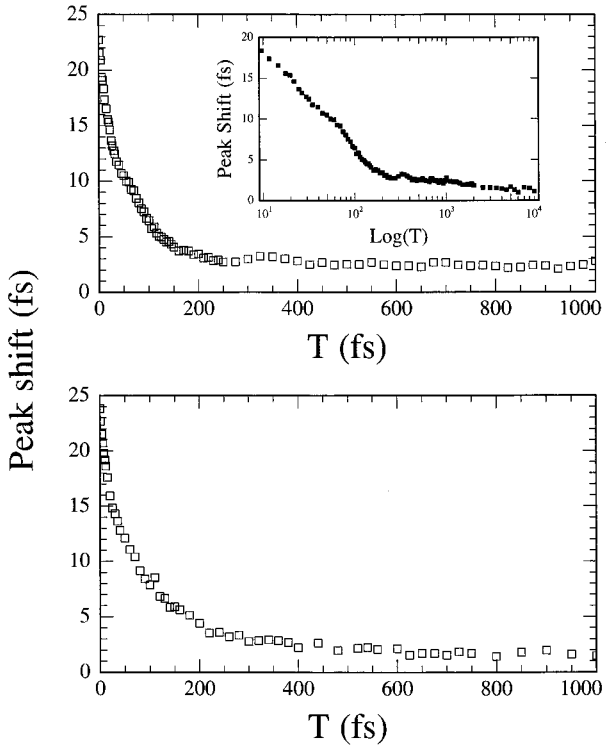

Figure 3. (top) Three-pulse echo peak shift of LH1 measured with 35 fs pulses centered at 870 nm. $\mathbf{k}_3$ at magic angle with respect to $\mathbf{k}_1$ and $\mathbf{k}_2$. The inset shows peak shift plotted vs log(T). This representation clearly reveals slow decay components. (bottom) Peak shift for LH2 measured with 35 fs pulses centered at 850 nm. $\mathbf{k}_3$ at magic angle with respect to $\mathbf{k}_1$ and $\mathbf{k}_2$. For the full-size plots, the size of the symbols indicates the approximate error bars for the peak shift values.

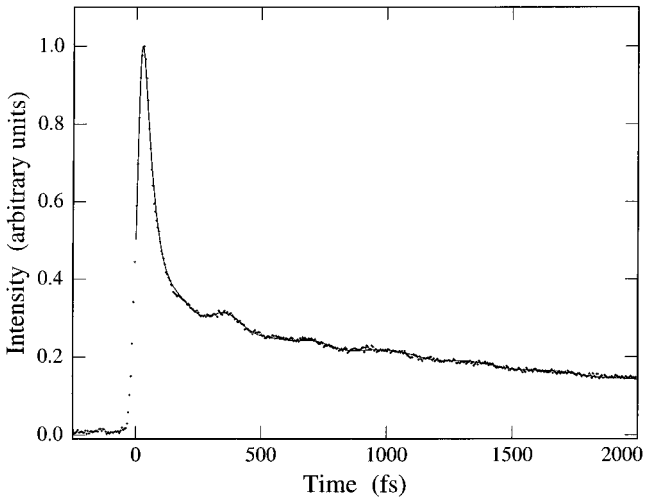

Figure 4. Dots represent LH1 transient grating signal measured with $\mathbf{k}_3$ at magic angle. The solid line is a fit, which includes convolution with the laser pulse. Fit parameters are given in the text.

The LH1 peak shift contains some oscillatory components; these oscillations are less discernible in the LH2 peak shift. In order to identify the oscillatory frequencies and damping times in the signals, we turn to the transient grating measurement, which is performed by temporally overlapping $\mathbf{k}_1$ and $\mathbf{k}_2$ and scanning $\mathbf{k}_3$. Shown in Figure 4 is the LH1 transient grating signal, along with a fit, which reveals 100 and 190 cm^{-1} oscillations with damping times of approximately 500 fs. The oscillation parameters were determined by linear prediction singular value decomposition.[39] The large "coherent spike"

hampers precise determination of the damping times and amplitudes. The transient grating signal also contains exponential decay components with time constants of 50 and 2300 fs.

1. Echo Simulation Methods. At this point we have identified the overall time scales of the peak shift decay. In order to discuss the underlying dynamics, we need to find a model *M(t)* that reproduces the observed peak shifts. We first describe here the approach used to calculate these signals in the case of noninteracting chromophores and then discuss modifications to this approach that we expect in the case of a mobile excited state.

At high temperatures, the starting point for simulations is usually *M(t)*, which in many cases can be written as a sum of Gaussian, exponential, and cosinusoidal terms,

$$M(t) = (\langle\Delta\omega_g{}^2\rangle e^{-(t/\tau_g)^2} + \sum_i \langle\Delta\omega_i{}^2\rangle e^{-t/\tau_i} + \sum_j \langle\Delta\omega_j{}^2\rangle e^{-t/\tau_j}\cos(\omega_j t + \phi))/\sum_k \langle\Delta\omega_k{}^2\rangle \quad (5)$$

where $\langle\Delta\omega^2\rangle$ is the coupling strength for each term (fluctuation amplitude).[32,43] In the high-temperature limit (the frequency of each mode, *not* its coupling strength, satisfies $\hbar\omega < kT$), the total amplitude of the fluctuations (the homogeneous line width) is related to the Stokes shift:

$$\text{Stokes shift} = \beta\sum_k \langle\Delta\omega_k{}^2\rangle \quad (6)$$

Later we will discuss the meaning of the "homogeneous width" more carefully. The linear and nonlinear spectroscopic signals are most conveniently calculated from the complex line shape function, *g(t)*:

$$g(t) = i\lambda\int_0^t dt_1\, M(t_1) + \langle\Delta\omega^2\rangle\int_0^t dt_1\int_0^{t_1} dt_2\, M(t_2) \quad (7)$$

In this expression, $M(0) = 1$. The absorption spectrum of the system can be calculated by taking the real part of the Fourier transform of $\exp[-g(t)]$:

$$\sigma_A(\omega) \propto \mathrm{Re}\int_{-\infty}^{\infty} dt\, e^{-i(\omega-\omega_{eg})t} e^{-g(t)} \quad (8)$$

where ω_{eg} is the average electronic transition frequency of the two-level system. The echo signals are calculated from $g(t)$ by formulating the nonlinear response functions:

$$R_1 (=R_4) = \exp[-g^*(t_1') + g(t_2') - g^*(t_3') - g(t_1'+t_2') - g(t_2'+t_3') + g^*(t_1'+t_2'+t_3')]$$

$$R_2 (=R_3) = \exp[-g(t_1') + g^*(t_2') - g^*(t_3') + g(t_1'+t_2') + g^*(t_2'+t_3') - g(t_1'+t_2'+t_3')]$$

$$R_5 (=R_8) = \exp[-g^*(t_1') + g^*(t_2') - g(t_3') - g^*(t_1'+t_2') - g^*(t_2'+t_3') + g^*(t_1'+t_2'+t_3')]$$

$$R_6 (=R_7) = \exp[-g^*(t_1') - g(t_2') - g(t_3') + g(t_1'+t_2') + g(t_2'+t_3') - g^*(t_1'+t_2'+t_3')] \quad (9)$$

which are used to calculate the third order polarization, $\mathbf{P}^{(3)}$:

$$\mathbf{P}^{(3)}(\tau,T,t') \propto \int_0^\infty dt_3'\int_0^\infty dt_2'\int_0^\infty dt_1' \sum_{i=0}^{4} R_i(t_1',t_2',t_3') \times \mathbf{E}_1{}^*(\mathbf{k}_1,t_1)\,\mathbf{E}_2{}^*(\mathbf{k}_2,t_2)\,\mathbf{E}_3{}^*(\mathbf{k}_3,t_3) \quad (10)$$

The $\mathbf{E}_i$ are the incident optical fields, with wave vector $\mathbf{k}_i$. The detected three-pulse echo signal is the modulus squared of $\mathbf{P}^{(3)}$ integrated over t', measured as a function of τ and T. Our simulations incorporate integration of the response functions over a Gaussian electric field envelope, whose fwhm reflects the experimental pulse duration. To simulate the peak shift, *M(t)* is used to calculate *g(t)*, which in turn is used to calculate the echo signal at various population delays (T). The peak of the signal at each T is then found with respect to τ. Each peak shift calculation takes about 30 min on a RISC-based workstation. The notation and computational methods used here are the same as those of ref 32.

Before discussing the set of parameters that reproduce the observed peak shift, it should be stated explicitly that we are modeling these data with the approach used for solvation dynamics, in the absence of a proper description for the effect of energy transfer on the echo signals. The Hamiltonian that gives rise to the aforementioned nonlinear response functions, formulated in terms of *M(t)*, does not include terms that induce chromophore electronic transitions (energy transfer) as a result of system−bath coupling.[43] However, in the limit of small electronic coupling between chromophores, it may still be possible to formulate the signal in terms of an *M(t)* that consists of a sum of exponential energy transfer terms with the usual system−bath dynamics. A plausible explanation for this approach was given in the Introduction. In addition, possible contributions from two-exciton states are neglected in the present analysis.

2. Echo Simulation Results. We begin by discussing the fit to the LH1 peak shift. First, we choose an *M(t)* consisting of Gaussian, exponential and oscillatory contributions and a static inhomogeneous distribution. In a three-pulse echo peak shift study of the B800 pigments in LH2, Joo *et al.* found that a 90 fs Gaussian with 100 cm^{-1} coupling strength reproduces the time scale of the initial decay.[44] In the absence of additional information, we take these values for the first component and attempt to vary the time scale and coupling strength to approximately match the initial phase of the LH1 peak shift. Next, we varied the coupling strengths and phases of the 110 and 190 cm^{-1} modes found in the transient grating measurement to match the oscillatory local maximum at $T \sim 350$ fs. A 12.5 ps exponential component (determined by fitting the peak shift directly) was added in order to reproduce the slow decay. Inclusion of the aforementioned terms results in two difficulties: the initial peak shift is overestimated by 50%, and its decay is too fast. Thus, the simulated absorption spectra were always too Gaussian, too wide, and did not reproduce the tail on the high-energy side of the experimental spectrum. These two problems were corrected by adding vibrations of 560 and 750 cm^{-1} to match the high-energy side of the spectrum and by adding an exponential (90 fs time constant, 160 cm^{-1} coupling strength) to match the decay. The rationale for these particular frequencies will be discussed in relation to LH2 (see below). Attempts to fit the fast decay only with a Gaussian rather than a dominant exponential component always result in overestimates of the absorption spectral width. Parameters were then adjusted slightly in order to improve the fits at $T > 50$ fs (for reasons to be discussed below, we find discrepancies at early times). The fit at early times is improved by decreasing the time scale of the Gaussian component from 90 fs down to 60 fs, but no improvement occurs for shorter time constants. The LH1 data and simulated peak shift are shown in Figure 5, along with *M(t)*. The simulated and observed spectra are shown in Figure 6. The values of the parameters for *M(t)* are contained in Table 1.

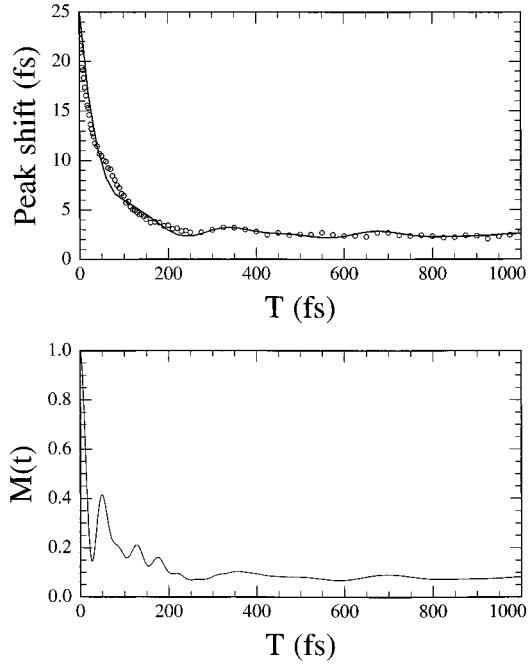

Figure 5. (top) LH1 experimental peak shift (symbols) and calculated (line) peak shift using 35 fs pulses. (bottom) Model *M(t)* used for the calculation.

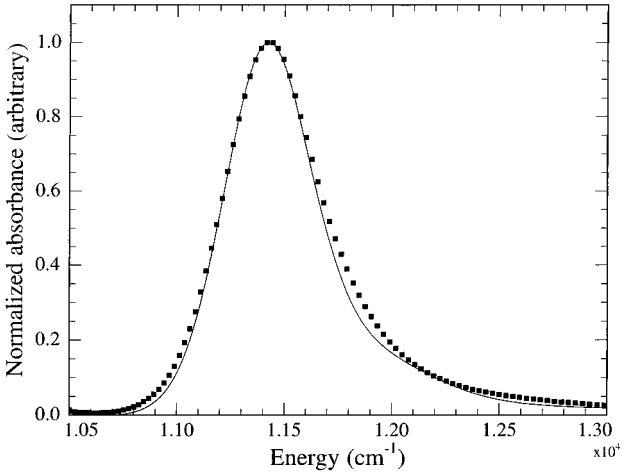

Figure 6. Measured (symbols) and simulated (line) absorption spectra for LH1. The simulated spectrum was calculated using the procedure described in the text, with $\omega_{eg} = 11\,320$ cm^{-1}.

TABLE 1: Parameters for LH1 Model *M(t)*; See Eq 4 for Definitions

	$\langle\Delta\omega^2\rangle^{1/2}$ (cm^{-1})	τ (fs)	ν (cm^{-1})	τ_{damp} (fs)	ϕ (rad)
Gaussian	100	60			
exponential	160	90			
exponential2	85	12500			
oscillation 1	45		110	700	−2.1
oscillation 2	45		190	400	0
oscillation 3	170		560	70	−0.2
oscillation 4	120		750	50	0

A similar procedure was performed in fitting the LH2 peak shift (data, fit, and *M(t)* are shown in Figure 7; the parameters are collected in Table 2). The slow phase of the decay is of smaller amplitude and longer time constant than in LH1. Also, the coupling strengths of the vibrations were decreased in order to account for their smaller amplitudes in the LH2 peak shift and transient grating signal. Furthermore, the frequencies of two excited state fundamental vibrations (750 and 920 cm^{-1}) determined by low-temperature hole-burning experiments were included in *M(t)*.[16] The coupling strengths were calculated from

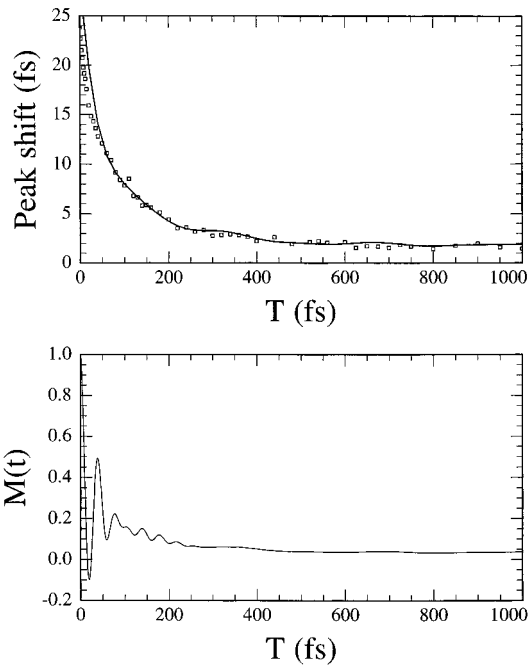

Figure 7. (top) LH2 experimental peak shift (symbols) and calculated peak shift using 35 fs pulses. (bottom) Model *M(t)* used for the calculation.

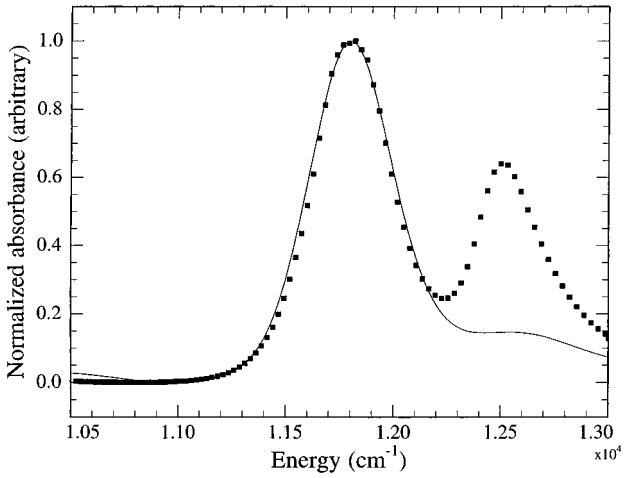

Figure 8. Measured (symbols) and simulated (line) absorption spectra for LH2. The simulated spectrum was calculated using the procedure described in the text, with $\omega_{eg} = 11\,710$ cm^{-1}.

TABLE 2: Parameters for LH2 Model *M(t)*; See Eq 4 for Definitions

	$\langle\Delta\omega^2\rangle^{1/2}$ (cm^{-1})	τ (fs)	ν (cm^{-1})	τ_{damp} (fs)	ϕ (rad)
Gaussian	80	40			
exponential	170	130			
exponential2	65	15000			
oscillation 1	30		110	700	−1.5
oscillation 2	30		190	400	0
oscillation 3	190		750	50	0
oscillation 4	190		920	50	0

the Franck−Condon factors (for the 0−1 transition) given in reference 16. The fit to the LH2 absorption spectrum (Figure 8) is rather good. Attempts to ascertain the quality of the fit are complicated by the B800 band on the high-energy side of the B850 peak, making it difficult to determine the shape of the B850 spectrum in this region in the absence of B800. However, mutant LH2 complexes are available which are thought to lack the binding site for B800.[26] The absorption spectra of these complexes are very similar to our simulated spectrum. Note that both our simulated line shapes and low-

temperature hole burning indicate the presence of B850 absorption in the B800 region. This absorption will facilitate B800 to B850 energy transfer by providing spectral overlap. Furthermore, this absorption will complicate the analysis of transient absorption measurements which assume that only B800 absorbs at these wavelengths.

Our model *M(t)* functions give estimated displacements between absorption and emission spectra of 212 and 160 cm^{-1} for LH1 and LH2, respectively. In order to determine the Stokes shift in the absence of energy transfer, one must remove the exponential components from consideration. In doing so, we obtain values of 70 cm^{-1} for LH1 and 40 cm^{-1} for LH2. Within a strongly coupled dimer model of B850 and B875, one would equate these Stokes shift values with those of the dimeric subunits comprising each ring. The observed displacement between absorption and emission maxima of the B820 subunit from *Rs. Rubrum* is 66 cm^{-1} at 77 K.[11] Recent pump−probe experiments by Kumble *et al.* on B820 have led to an estimate of the value of the Stokes shift of ∼80 cm^{-1}.[40] For comparison, the Stokes shift of Bchl dissolved in cyclohexanol has been measured to be 260 cm^{-1}.[36] The remaining portion of the shift due to the exponential components can be loosely associated with the spectral equilibration due to energy transfer. The magnitude of these shifts are 140 cm^{-1} for LH1 and 120 cm^{-1} for LH2. The value for LH1 is in good agreement with that observed for spectral equilibration in broad-band pump−probe measurements and with the value of spectral shift expected from room temperature equilibration of a 500 cm^{-1} fwhm distribution of pigment energies.[24] Another contribution to the Stokes shift which may be important is that arising from relaxation among the exciton levels of the aggregate. Recently, Meier *et al.* have estimated this shift to be 139 cm^{-1}.[4] Later, we will consider the consequences of the magnitude of the Stokes shift on the electronic level structure of the Bchl aggregates.

The fast (40−60 fs) Gaussian component in *M(t)* comes from rapid fluctuations of the protein environment, a process that we choose to call homogeneous broadening. Of course, there are many points of view on the meaning of "homogeneous", but we state here a definition that suffices for a clear discussion in the present inquiry. In this view, the absorption spectrum is composed of intramolecular vibrational lines, each of which is broadened by the dynamical processes of the medium (in this case, the protein). The fluctuations of the protein are of sufficiently low frequency that they are thermally active, thus satisfying the fluctuation−dissipation theorem; under these conditions the homogeneous line width is related to the Stokes shift as stated in eq 5. To make this definition clear, we restate the point: the homogeneous line width is only that caused by the dynamics (vibrations) of the protein or solvent environment. Thus, the coupling strength of the Gaussian component in *M(t)*, multiplied by $\sqrt{(8 \ln 2)}$, is the fwhm of the homogeneous line width. Implicit in our definition is the assumption that we can somehow distinguish between the vibrational modes of the chromophore and those of the environment. This distinction cannot be made by an examination of *M(t)*, because all modes are added in the same manner. Therefore, another possible definition for the fwhm of the homogeneous line width, which includes all thermally active modes, is the sum of the coupling strengths for all modes with frequencies $< kT$, multiplied by $\sqrt{(8 \ln 2)}$. In order to clarify the upcoming discussion, we designate this quantity Γ, the thermal fluctuation width.

Our results place an upper limit of 60 fs on the time constant for the Gaussian process in *M(t)*. A lower limit cannot be assigned, because the simulated peak shift is not sensitive to further decrease in the time constant below ∼60 fs. As discussed above, the coupling strength for this component is equal to the second moment of the homogeneous line width. The LH1 and LH2 homogeneous line widths resulting from the model are 235 and 188 cm^{-1} fwhm, respectively. The coupling strengths of these Gaussian components in LH1 and LH2 are similar to the value found for the B800 pigments in a previous three-pulse echo study, but much smaller than found for dyes in polar solvents such as acetonitrile or ethanol.[32,37,38,44]

The 110 and 190 cm^{-1} oscillations from the LH1 transient grating and peak shift are similar frequencies to those observed in pump−probe experiments by Sundström and co-workers.[25] In single-color (870 nm) transient absorption measurements at 4.2 K, they found 90, 110, 180, and 300 cm^{-1} vibrations with 300−500 fs damping times. These oscillations were found to persist up to room temperature. The amplitude of the oscillations was found to be much smaller in LH2 and seemed to be dominated by one of the same frequencies (110 cm^{-1}) with a similar damping time. Our *M(t)* for LH2 reflects these observations, by having smaller coupling strengths for the vibrations as compared to LH1, but using the same damping times. The present transient-grating and three-pulse echo measurements are unable to distinguish between ground and excited state vibrations; however, fluorescence up-conversion measurements on LH1 confirm the 110 cm^{-1} oscillation as originating from excited state motion.[12]

Although 560 and 750 cm^{-1} oscillations were not observed in the LH1 transient grating or peak shift measurements, we have included these modes so as to model the effect of hard to detect vibrational structure in *M(t)*. High-frequency modes reduce the simulated $T = 0$ value of the peak shift and reproduce the high-energy region of the LH1 absorption spectrum. Evidence for high-frequency modes strongly coupled to B850 Q_y absorption has been found by Small and co-workers, who find 750 and 920 cm^{-1} vibronic holes in 4.2 K hole-burning measurements on LH2.[15] Since our signals do not contain oscillations at these frequencies, we cannot determine amplitudes, damping times, and phases. For LH2, we include these modes with coupling strengths determined from their Franck−Condon factors. We do not have hole-burning data for LH1, so we reduce the coupling strength of the 750 cm^{-1} mode and add a 560 cm^{-1} vibration, which is found in both low-temperature emission spectra of Bchl[42] and hole burning of B850.[15] The 50−70 fs damping times we use for these high-frequency vibrations are unrealistically short for dephasing of a single mode. However, there are likely to be several vibrational modes clustered at each frequency. For example, high-resolution emission spectra of Bchl in glasses at low temperature resolve three modes near 920 cm^{-1}.[42] It follows that fast damping times should be interpreted as the dephasing between various modes at each frequency range. We suggest that the remaining discrepancy between the simulated and observed peak shifts results from unresolved vibrational structure. Identifying these vibrations so as to fit the echo signal precisely at early times ($T < 50$ fs) is probably not crucial for the discussion on the effects of energy transfer on the echo signals. As we can see from these deliberations, knowledge of the chromophore vibrational structure is important for interpretation of the 3PEPS experiment.[32,33,37,38] Work to assess the importance of nonimpulsively excited vibrations on the three-pulse echo peak shift is still in progress.

There are several possible explanations for the exponential time components in the LH1 and LH2 peak shifts. The 90 and 130 fs components in the model *M(t)* functions for LH1 and LH2 may result from vibrational relaxation, protein reorganization (solvation), or spectral diffusion. Moreover, since these processes are not independent, the time constants themselves need not correspond to any one of these processes separately.

However, large-amplitude exponential components on this time scale have not been previously found in *M(t)* for dye molecules in solutions or glasses, nor has this been found in *M(t)* for the B800.[32,34,38,44] These time constants are very similar to the hopping times found by modeling the depolarization and spectral equilibration processes in LH1 and LH2.[12,13,23,24] In addition, the dominance of these components in *M(t)* for systems whose major characteristic is efficient, ultrafast energy transfer suggests that they are signatures of the energy transfer process. The longer time scale (12.5 and 15 ps) components in *M(t)* may also result from the hopping process, because energy transfer within an inhomogeneously broadened band is expected to occur on multiple time scales. For example, depolarization simulations of LH2 with a 500 cm^{-1} inhomogeneous distribution are well fit by a biexponential decay with time constants ~100 fs (66%) and 1 ps (33%). The relative amplitude of these two contributions is very similar to those of the exponential components in *M(t)*. Although this possibility was not discussed at that time, an exponential component in *M(t)* that is similar to the time constant of an excitation transfer process was found in our laboratory's 3PEPS study of B800.[44] The peak shift shows a 600 fs exponential component in accord with the B800 to B800 transfer time measured in transient absorption experiments.[9] Thus, it is reasonable to suppose that the excitation transfer times are manifested in *M(t)* as exponential components. These factors lead us to propose that the exponential decays in our model *M(t)* functions reflect the site to site excitation transfer time scales.

As discussed in the Introduction, finite residual values of $\tau^*(T\rightarrow\infty)$ may result from a static inhomogeneous distribution of the chromophores. If the 400−500 cm^{-1} values of static inhomogeneous broadening suggested by previous experiments were to be included in our simulations, $\tau^*(T\rightarrow\infty)$ values of 5−7 fs would result.[12,13,23] In the presence of energy transfer, the distribution of site energies underlying the absorption spectrum may be significantly larger than indicated by a residual peak shift. Therefore, our finding that $\tau^*(T\rightarrow\infty)$ is close to zero for B850 and B875 should not be taken to mean that there is no static distribution of pigment energies. The relationship between values of $\tau^*(T\rightarrow\infty)$ and the extent of inhomogeneous broadening in the presence of energy transfer needs to be clarified by further theoretical efforts. As mentioned in the Introduction, we may estimate the width of the distribution in the B850 and B875 bands by calculating the homogeneous line widths determined by *M(t)* and assuming the rest of the spectral width to be the result of inhomogeneous broadening. This approach neglects the possibility that some of the remaining bandwidth is excitonic and therefore places an upper limit on the inhomogeneous bandwidths. For LH1, the observed room temperature spectrum has a width of 580 cm^{-1} fwhm, whereas the homogeneous line width determined by this work is 235 cm^{-1}. Assuming a Gaussian distribution of site energies, the required value for consistency with the spectrum is, therefore, 530 cm^{-1} fwhm. Similarly, the B850 room temperature spectrum has a width of 430 cm^{-1} fwhm. The homogeneous line width of 188 cm^{-1} implies an inhomogeneous distribution of 390 cm^{-1} fwhm. As discussed earlier, the simplest way to include the effect of energy migration on the value of $\tau^*(T\rightarrow\infty)$ is to regard the inhomogeneous width contribution to the peak shift as being time dependent. To pursue this point and in order to assess the magnitude and time scale of changes in the inhomogeneous width, we will describe simulations based on Förster energy transfer in rings (see below). Clearly, a more satisfactory approach would be to reformulate the description of the 3PEPS experiment to include energy migration between chromophores. We will first consider whether our results are consistent with the hopping approach.

3. Localized vs Delocalized Models. The elements that determine the extent of electronic delocalization are the magnitude of electronic coupling between chromophores, static inhomogeneous broadening, and the coupling of the electronic transition to nuclear degrees of freedom. When the magnitude of the electronic coupling becomes outweighed by the last two factors, the electronic states will become localized. The values of inhomogeneous broadening determined here (400−500 cm^{-1}) are similar to those found from modeling the nonexponential depolarizations observed in B875 and B850.[12,13] In those studies, use of the hopping model was partially justified with an exciton level calculation (diagonalization of the Hamiltonian) which shows that a 200 cm^{-1} (fwhm) distribution of site energies will localize excitations on the low-energy side of the absorption spectrum to ~4 pigments. Taken by themselves, the larger values of inhomogeneous broadening found here will lead to a greater degree of localization than calculated in those simulations. At this point, we will consider the effects of vibrations along with inhomogeneous broadening.

In addition to disorder, both intramolecular and intermolecular nuclear degrees of freedom will localize the electronic states. A rigorous treatment of localization by vibrations is a very complicated problem[45−48] that we will not attempt to pursue here. We only show that the thermal fluctuation width is comparable to the electronic coupling in these complexes and that significant localization ensues. Our results show that fast fluctuations (on a 50 fs time scale) make significant contributions to *M(t)* for LH1 and LH2. Some of the fast decay is the result of optically excited, high-frequency vibrations. We focus attention on the effect of fluctuations in the high-temperature limit ($\hbar\omega < kT$) because only thermally active modes should be considered. As discussed above, we are excluding the exponential components and the vibrations with frequencies >200 cm^{-1} (see Tables 1 and 2) to calculate the thermal fluctuation amplitude. We find $\Gamma = 447$ cm^{-1} for LH1 and 239 cm^{-1} for LH2. These values are comparable to the magnitude of the electronic coupling in B850, as estimated by point−monopole calculations ($J \sim 250$ cm^{-1}).[13,20] Next, we utilize Leegwater's approach as a means of estimating the combined effect of fluctuations and disorder.[22] In that work, the effect of vibrations is represented by Γ. Furthermore, our results show that the standard deviation of the inhomogeneous line width (Δ) is 530 $cm^{-1}/\sqrt{8 \ln 2}$, or 226 cm^{-1}. Summarizing our results, we have $\Gamma/J \sim 2$, and $\Delta/J \sim 1$, which implies an excitation localized on 3−4 pigments (see Figure 6 of ref 22). Similar considerations hold for B850. An important consequence of our analysis is the finding that the vibrational coupling strengths outweigh the electronic coupling in LH1 and LH2; i.e., *the electronic states are dynamically localized.*

Kumble *et al.* take a similar view of the issue of dynamic localization.[40] In their study, the time scale of the B820 Stokes shift is evident in their experiment as a 20 fs movement of the nuclear wavepacket, which causes both a shift in their frequency-resolved transient absorption signals and a fast decay component in the anisotropy. These vibrational dynamics contribute to the initial decay of the peak shift; both measurements reveal the time scale of the same process.[34] This time scale of the Stokes shift is much shorter than the estimated hopping times in B850 and B875 (see below). As a consequence, even if the electronic state initially prepared by a short optical pulse is delocalized over many Bchl, it will rapidly localize onto 3−4 pigments, so that a weak-coupling approach should be appropriate at times ≳50 fs. Kumble and co-workers note that the 80 cm^{-1} B820 Stokes shift implies a 300 cm^{-1} homogeneous line width and

point out that the excited states of LH1 must be localized unless the value of the electronic coupling is significantly larger than 300 cm^{-1}. As indicated by this discussion, recent results on the subject of localization in antenna systems provide more impetus for the view that excitation transfer within B850 and B875 can be modeled well with dimeric excitations.

4. Relation to Previous Work; Fluorescence Depolarization. When using the hopping model, the ~100 fs decay process in *M(t)* may be interpreted as follows: In the absence of site−energy correlations between neighboring pigments, "hopping" on an inhomogeneously broadened ring will cause a decay of *M(t)* on time scales related to the hopping time. More specifically, *M(t)* will track the probability that the excitation remains on the initially excited pigment (and electronic state). In the case of a homogeneous system, the rate matrix for a ring with only nearest-neighbor hopping can be diagonalized analytically, revealing multiexponential behavior.[49] When approximating this multiexponential decay with a biexponential function, the major component is approximately half the hopping time. Within this interpretation of *M(t)*, the 90 fs decay of *M(t)* in LH1, for example, indicates a hopping time of ~180 fs. For an inhomogeneous ring, one has to resort to Monte Carlo calculations; however, the fast lifetimes will fall between $\tau_{hop}/2$ and τ_{hop}. For rings larger than four sites, these conclusions are not sensitive to the ring size; the ring size mainly affects the amplitudes of the slower components. Numerical simulations and more detailed discussion of these results will be presented in a separate paper.[50]

We can also estimate the homogeneous transfer time using Förster theory. The values for the B850 and B875 Stokes shifts and homogeneous line shapes are taken from the present work. For excitation transfer on the time scale of the vibrational dynamics, the use of the homogeneous line shape for the overlap integral is problematic;[10] use of the strong-coupling or intermediate-coupling cases is more appropriate. However, we will use the weak-coupling formula simply as an estimate of the hopping time scales. The integrated transition dipole strength of the Bchl dimer is taken to be 77 D^2.[12] LH1 is modeled as a 96 Å diameter ring of 16 dimers whose transition dipoles are tangential to the ring.[6] The B850 pigments are modeled as a 52 Å diameter ring of nine dimers whose transition dipoles are tilted 22° with respect to the ring. This arrangement is consistent with the 2.5 Å crystal structure of LH2 from *Rps. acidophila*.[4] The homogeneous hopping times, as calculated from Förster theory, are 75 and 80 fs for B875 and B850, respectively. These hopping times give depolarization times of 128 and 50 fs for B875 and B850, respectively. These depolarization time scales are in reasonable agreement with those found in refs 12 and 13. The estimate of the LH1 depolarization time is slightly longer than the dominant value found in ref 12. Part of this discrepancy may result from the assumption of a 16-dimer ring for LH1; smaller rings would lead to better agreement. Both time-resolved annihilation experiments[12] and two-dimensional diffraction studies[6] have shown evidence for smaller rings.

These considerations indicate that the dimer-to-dimer hopping model, utilized with the parameters determined by this echo study, is consistent with previous work on the B850 and B875 bands. In particular, the hopping times and inhomogeneous bandwidths resulting from our model are consistent with earlier studies.[12,13,24] The most likely explanation for the exponential decay time scales in *M(t)*, therefore, seems to be the decay of population from the initially excited chromophores. It is striking that the *M(t)* functions for B850 and B875, in contrast with those for chromophores in solvents and glasses, decay so rapidly.[32,37,38] We suggest that longer time scale dynamics are inaccessible to the B850 and B875 3PEPS measurements because the ability for the system to rephase is lost on the time scale of the fast hopping process. We will look for the slower protein contributions to *M(t)* in these antenna complexes by performing these same experiments on the isolated B820 dimer from the LH1 antenna.

IV. Concluding Remarks

We summarize our findings on the parameters underlying B875 and B850 dynamics, based on the model *M(t)* functions that reproduce the peak shifts and absorption spectra: For LH1 we find a homogeneous line width of 235 cm^{-1}, an inhomogeneous line width of 530 cm^{-1}, a Stokes shift of 212 cm^{-1}, and an electronic origin (0−0 transition) at 11 320 cm^{-1}. For LH2 we find a homogeneous line width of 188 cm^{-1}, an inhomogeneous line width of 390 cm^{-1}, a Stokes shift of 165 cm^{-1}, and an electronic origin at 11 710 cm^{-1}. In both cases, we do not include the presence of multiple exciton states; the inhomogeneous line widths should thus be considered upper limits. For both LH1 and LH2 we find high-frequency vibrational modes to be of importance for simulating the peak shift and absorption spectra. In the case of LH2, we include 750 and 920 cm^{-1} vibrations observed in B850 hole-burning studies.[16] For LH1, we model the influence of nonimpulsively excited vibrations by using frequencies of 560 and 750 cm^{-1}. The thermally active vibrational modes, in combination with the Gaussian homogeneous process in *M(t)*, serve to dynamically localize the electronic states in B850 and B875. The model *M(t)*s reveal that rapid fluctuations of magnitude comparable to the electronic coupling are present in B850 and B875. We followed a simplified treatment to provide an estimate for the combined effects of static disorder and thermally active vibrations and find the electronic states localized onto 3−4 Bchl.[22] Finally, we show that the hopping model, when applied to LH1, is consistent with previous time-resolved experimental results. Similar results hold for LH2.

The *M(t)* functions for B850 and B875 will be of use as input to theoretical treatments of energy transfer that utilize a spectral density to model the coupling between the electronic and nuclear degrees of freedom.[51−53] Of course, a formal theoretical framework for the effect of energy transfer on the echo signal remains to be developed. Challenges for a description of the echo signal in the presence of energy transfer include the need to account for the progressive loss of rephasing due to incoherent hopping, input of the excitation conditions, evolution of the inhomogeneous distribution, and multiple excitonic states. The collective oscillator density matrix approach very recently presented by Meier *et al.* provides a framework for the description of these dynamics.[41] At present, this approach is able to consistently explain both the temperature-dependent superradiance[21] and pump−probe experiments.[19] The current experimental results provide further evidence that vibrational coherence transfer is at work in LH1 and LH2, because the hopping times derived from the model are much shorter than the dephasing of the coherences for the 110 and 190 cm^{-1} vibrational modes. The study of coherence transfer in LH1 and LH2 is an important direction for the future. We conclude by noting that the total magnitude of the fluctuations $\langle \Delta\omega^2 \rangle$ for B850 and B875 (as judged by their Stokes shifts and homogeneous line widths) is much smaller than that observed for dyes in polar solvents or glasses in similar studies. In comparison, the electronic transitions of Bchl in light-harvesting systems seem to be more weakly coupled both to fluctuations in the protein environment and to intramolecular vibrations. This weak system−bath coupling is likely to be one of the most important factors underlying the efficiency of the energy transfer processes in LH1 and LH2 complexes.

Acknowledgment. This work was supported by the U.S. National Science Foundation. We thank S. N. Dikshit for preparing the detergent-isolated LH1 and LH2 complexes. We would also like to thank Minhaeng Cho, Taiha Joo, Jan Adrien Leegwater, and Rienk van Grondelle for many helpful discussions. R.J. acknowledges a graduate fellowship from the National Physical Science Consortium. F.v.M. was supported in Chicago by a Talent Fellowship from the NWO.

References and Notes

(1) Van Grondelle, R.; Dekker, J. P.; Gilbro, T.; Sundström, V. *Biochim. Biophys. Acta* **1994**, *1187*, 1.
(2) Kühlbrandt, W. *Nature* **1995**, *374*, 497.
(3) McDermott, G.; Prince, S. M.; Freer, A. A.; Hawthornthwaite-Lawless, A. M.; Papiz, M. Z.; Cogdell, R. J.; Isaacs, N. W. *Nature* **1995**, *374*, 517.
(4) Cogdell, R. J. Private communication.
(5) Koepke, J.; Hu, X.; Muenke, C.; Schulten, K.; Michel, H. *Structure* **1996**, *4*, 581.
(6) Karrasch, S.; Bullough, P. A.; Ghosh, R. *EMBO J.* **1995**, *14*, 631.
(7) Trautman, J. K.; Shreve, A. P.; Violette, C. A.; Frank, H. A.; Owens, T .G.; Albrecht, A. C. *Proc. Natl. Acad. Sci. U.S.A.* **1990**, *87*, 215.
(8) Hess, S.; Feldchtein, F.; Babin, A.; Nurgaleev, I.; Pullerits, T.; Sergeev, A.; Sundström, V. *Chem. Phys. Lett.* **1993**, *216*, 247.
(9) Monshouwer, R.; Ortiz de Zarate, I.; van Mourik, F.; van Grondelle, R. *Chem. Phys. Lett.* **1995**, *246*, 341.
(10) Förster, T. Modern Quantum Chemistry; Academic Press: New York, 1965; Vol. III, pp 93−137.
(11) Visschers, R. W.; Chang, M. C.; van Mourik, F.; Parkes-Loach, P. S.; Heller, B. A.; Loach, P. A.; van Grondelle, R. *Biochemistry* **1991**, *30*, 5734.
(12) Bradforth, S. E.; Jimenez, R.; van Mourik, F.; van Grondelle, R.; Fleming, G. R. *J. Phys. Chem.* **1995**, *99*, 16179.
(13) Jimenez, R.; Dikshit, S. N.; Bradforth, S. E.; Fleming, G. R. *J. Phys. Chem.* **1996**, *100*, 6825.
(14) Fidder, H.; Knoester, J.; Wiersma, D. A. *J. Chem. Phys.* **1991**, *95*, 7880.
(15) Reddy, N. R. S.; Picorel, R.; Small, G. J. *J. Phys. Chem.* **1992**, *96*, 6458.
(16) Reddy, N. R. S.; Small, G. J.; Seibert, M.; Picorel, R. *Chem. Phys. Lett.* **1991**, *181*, 391.
(17) Kennis, J. T. M.; Streltsov, A. M.; Aartsma, T. J.; Nozawa, T.; Amesz, J. *J. Phys. Chem.* **1996**, *100*, 2438.
(18) Pullerits, T.; Sundström, V. *Acc. Chem. Res.* **1996**, *29*, 381.
(19) Pullerits, T.; Chachisvilis, M.; Sundström, V. *J. Phys. Chem.* **1996**, *100*, 10787.
(20) Sauer, K.; Cogdell, R. J.; Prince. S. M.; Freer, A. A.; Isaacs, N. W.; Scheer, H. *Photochem. Photobiol.* **1996**, *64*, 564.
(21) Monshouwer, R.; Abrahamsson, M.; van Mourik, F.; van Grondelle, R. *J. Phys. Chem. B* **1997**, *101*, 7241.
(22) Leegwater, J. A. *J. Phys. Chem.* **1996**, *100*, 14403.
(23) Visser, H. M.; Somsen, O. J. G.; van Mourik, F.; Lin, S.; van Stokkum, I.; van Grondelle, R. *Biophys. J.* **1995**, *69*, 1083.
(24) Visser, H. M.; Somsen, O. J. G.; van Mourik, F.; van Grondelle, R. *J. Phys. Chem.*, in press.
(25) Chachisvilis, M.; Pullerits, T.; Jones, M. R.; Hunter, C. N.; Sundström, V. *Chem. Phys. Lett.* **1994**, *224*, 345.
(26) Visschers, R. W.; Crielaard, W.; Fowler, G. J. S.; Hunter, C. N.; van Grondelle, R. *Biochim. Biophys. Acta* **1994**, *1183*, 483.
(27) Jean, J. M.; Friesner, R. A.; Fleming, G. R. *J. Chem. Phys.* **1992**, *96*, 5927.
(28) Jean, J. M. *J. Chem. Phys.* **1994**, *101*, 10464.
(29) Jean, J. M.; Fleming, G. R. *J. Chem. Phys.* **1995**, *103*, 2092.
(30) Bergström, H.; van Grondelle, R.; Sundström, V. *FEBS Lett.* **1989**, *250*, 503.
(31) Beekman, L. M. P.; van Mourik, F.; Jones, M. R.; Visser, H. M.; Hunter, C. N.; van Grondelle, R. *Biochemistry* **1994**, *33*, 3143.
(32) Joo, T.; Jia, Y.; Yu, J.; Lang, M. J.; Fleming, G. R. *J. Chem. Phys.* **1996**, *104*, 6089.
(33) De Boeij, W.; Psenichnikov, M. S.; Wiersma, D. A. *Chem. Phys. Lett.* **1996**, *253*, 53.
(34) De Boeij, W.; Psenichnikov, M. S.; Wiersma, D. A. *Chem. Phys. Lett.* **1995**, *238*, 1.
(35) Cho, M.; Yu, J.; Joo, T.; Nagasawa, Y.; Passino, S.; Fleming, G. R. *J. Phys. Chem.* **1996**, *100*, 11944.
(36) Bolt, J. D.; Sauer, K. *Biochim. Biophys. Acta* **1981**, *637*, 342.
(37) Nagasawa, Y.; Passino, S. A.; Joo, T.; Fleming, G. R. *J. Chem. Phys.* **1996**, *106*, 4840.
(38) Passino, S. A.; Nagasawa, Y.; Joo, T.; Fleming, G. R. *J. Phys. Chem. A* **1997**, *101*, 725.
(39) Wise, F. W.; Rosker, M. J.; Millhauser, G. L.; Tang, C. L. *IEEE J. Quantum Electron.* **1987**, *QE-23*, 1116.
(40) Kumble, R.; Palese, S.; Visschers, R. W.; Dutton, P. L.; Hochstrasser, R. M. *Chem. Phys. Lett.* **1996**, *261*, 396.
(41) Meier, T.; Chernyak, V.; Mukamel, S. *J. Phys. Chem. B* **1997**, *101*, 7332.
(42) Renge, I.; Mauring, K.; Avaarma, R. *J. Lumin.* **1987**, *37*, 207.
(43) Mukamel, S. *Principles of Nonlinear Spectroscopy*; Oxford University Press: New York, 1995.
(44) Joo, T.; Jia, Y.; Yu, J.; Jonas, D. M.; Fleming, G. R. *J. Phys. Chem.* **1996**, *100*, 2399.
(45) Holstein, T. *Ann. Phys. (N.Y.)* **1959**, *8*, 325.
(46) Toyozawa, T. *Prog. Theor. Phys.* **1961**, *26*, 29.
(47) Friesner, R. A.; Silbey, R. *J. Chem. Phys.* **1981**, *75*, 3925.
(48) Spano, F. C.; Kuklinski, J. R.; Mukamel, S. *Phys. Rev. Lett.* **1990**, *65*, 211.
(49) Matthieu Visser, Ph.D. Thesis, Vrije University, Amsterdam, The Netherlands.
(50) van Mourik, F.; Jimenez, R.; Fleming, G. R. Manuscript in preparation.
(51) Egger, R.; Mak, C. H. *J. Phys. Chem.* **1994**, *98*, 9903.
(52) Schulten, K.; Tesch, M. *Chem. Phys.* **1991**, *158*, 421.
(53) Chernyak, V.; Mukamel, S. *J. Chem. Phys.* **1996**, *105*, 4565.